

AD-A199 103

OFFICE OF NAVAL RESEARCH  
Research Contract N00014-87-K-0014  
R&T Code 413E026---01

Technical Report No. 11

ELECTRICAL RESISTIVITY, MAGNETIC SUSCEPTIBILITY, THERMOELECTRIC  
POWER AND HEAT CAPACITY OF PtGa<sub>2</sub>

by

L. Hsu, L.W. Zhou, F.L.A. Machado,

Department of Physics  
and Solid State Sciences Center

and

R. Stanley Williams

Department of Chemistry & Biochemistry  
and Solid State Sciences Center  
University of California, Los Angeles, CA 90024-1569

Submitted for publication in  
*Physical Review B*

University of California, Los Angeles  
Department of Chemistry & Biochemistry  
and Solid State Sciences Center  
Los Angeles, CA 90024-1569

July, 1988

Reproduction in whole or part is permitted for  
any purpose of the United States Government.

This document has been approved for public release and sale;  
its distribution is unlimited

DTIC  
ELECTE  
AUG 04 1988  
S D  
& H

## REPORT DOCUMENTATION PAGE

1a REPORT SECURITY CLASSIFICATION UNCLASSIFIED			1b RESTRICTIVE MARKINGS N/A		
2a SECURITY CLASSIFICATION AUTHORITY N/A			3. DISTRIBUTION / AVAILABILITY OF REPORT Approved for public release; distribution unlimited		
2b DECLASSIFICATION / DOWNGRADING SCHEDULE N/A					
4 PERFORMING ORGANIZATION REPORT NUMBER(S) N/A			5. MONITORING ORGANIZATION REPORT NUMBER(S)		
6a NAME OF PERFORMING ORGANIZATION The Regents of the University of California		6b OFFICE SYMBOL (if applicable)	7a NAME OF MONITORING ORGANIZATION 1) ONR Pasadena - Administrative 2) ONR Alexandria - Technical		
6c ADDRESS (City, State, and ZIP Code) Office of Contracts & Grants Administration U C L A, 405 Hilgard Avenue Los Angeles, CA 90024			7b ADDRESS (City, State, and ZIP Code) 1) 1030 E. Green Street, Pasadena, CA 91106 2) 800 N. Quincy St., Arlington, VA 22217-5000		
8a NAME OF FUNDING / SPONSORING ORGANIZATION Office of Naval Research		8b OFFICE SYMBOL (if applicable) ONR	9 PROCUREMENT INSTRUMENT IDENTIFICATION NUMBER N00014-87-K-0014		
8c ADDRESS (City, State, and ZIP Code) 800 N. Quincy Street, 614A:DHP Arlington, VA 22217-5000			10 SOURCE OF FUNDING NUMBERS	PROGRAM ELEMENT NO	PROJECT NO
			TASK NO	WORK UNIT ACCESSION NO	
11 TITLE (Include Security Classification) UNCLASSIFIED: Tech Rept. #11 ELECTRICAL RESISTIVITY, MAGNETIC SUSCEPTIBILITY, THERMO- ELECTRIC POWER AND HEAT CAPACITY OF PtGa <sub>2</sub>					
12 PERSONAL AUTHOR(S) L. Hsu, L.W. Zhou, F.L.A. Machado and R.S. Williams					
13a TYPE OF REPORT Technical Preprint		13b TIME COVERED FROM Aug '87 TO July '88	14. DATE OF REPORT (Year, Month, Day) 1988: July 22		15 PAGE COUNT 8 + Refs & Figs
16 SUPPLEMENTARY NOTATION					
17. COSATI CODES			18 SUBJECT TERMS (Continue on reverse if necessary and identify by block number) intermetallic compound, diamagnetic susceptibility, density of states, transport properties, band structure,		
FIELD	GROUP	SUB-GROUP			
19. ABSTRACT (Continue on reverse if necessary and identify by block number) The electrical resistivity ( $\rho$ ), magnetic susceptibility ( $\chi$ ), thermoelectric power ( $S$ ), and specific heat ( $C_p$ ) of PtGa <sub>2</sub> were measured as a function of temperature ( $T$ ). The metallic behavior of this intermetallic compound is shown from the room temperature resistivity value (190 $\Omega$ -cm) and the linear dependence of the $S$ vs. $T$ curve at temperatures above the Debye temperature ( $\theta_D$ ). The diamagnetic susceptibility is independent of $T$ . The density of states (DOS) at the Fermi energy ( $E_F$ ) obtained from $\chi$ and $S$ data agree within 22% and 15%, respectively, of the value obtained previously from a semiempirical band structure calculation. The low temperature $C_p$ data, however, yielded a much smaller DOS at $E_F$ . The data for PtGa <sub>2</sub> are compared to those for Au and AuGa <sub>2</sub> in order to better understand the transport properties of this material.					
20 DISTRIBUTION / AVAILABILITY OF ABSTRACT <input checked="" type="checkbox"/> UNCLASSIFIED/UNLIMITED <input type="checkbox"/> SAME AS RPT <input type="checkbox"/> DTIC USERS			21 ABSTRACT SECURITY CLASSIFICATION UNCLASSIFIED		
22a NAME OF RESPONSIBLE INDIVIDUAL R. Stanley Williams			22b TELEPHONE (include Area Code) (213) 825-8818	22c OFFICE SYMBOL UCLA	

**Electrical Resistivity, Magnetic Susceptibility, Thermoelectric Power,  
and Specific Heat of PtGa<sub>2</sub>**

Li-Shing Hsu, Lu-Wei Zhou,<sup>a)</sup> F. L. A. Machado,<sup>b)</sup>  
Department of Physics and Solid State Science Center,  
University of California, Los Angeles, California 90024

and

R. Stanley Williams  
Department of Chemistry and Biochemistry and Solid State Science Center, University of  
California, Los Angeles, California 90024-1569

The electrical resistivity ( $\rho$ ), magnetic susceptibility ( $\chi$ ), thermoelectric power ( $S$ ), and specific heat ( $C_p$ ) of PtGa<sub>2</sub> were measured as a function of temperature ( $T$ ). The metallic behavior of this intermetallic compound is shown from the room temperature resistivity value ( $19\mu\Omega\text{-cm}$ ) and the linear dependence of the  $S$  vs.  $T$  curve at temperatures above the Debye temperature ( $\theta_D$ ). The diamagnetic susceptibility is independent of  $T$ . The density of states (DOS) at the Fermi energy ( $E_F$ ) obtained from  $\chi$  and  $S$  data agree within 22% and 15%, respectively, of the value obtained previously from a semiempirical band structure calculation. The low temperature  $C_p$  data, however, yielded a much smaller DOS at  $E_F$ . The data for PtGa<sub>2</sub> are compared to those for Au and AuGa<sub>2</sub> in order to better understand the transport properties of this material.

-----  
a) Permanent address: Physics Department, Fudan University, Shanghai, China.

b) Permanent address: Universidade Estadual de Campinas, Instituto de Fisica "Gleb Wataghin",  
Departamento de Fisica do Estado Solido e Ciencia dos Materiais, Caixa Postal 6165,  
Campinas, SP 13081, Brasil.

## I. Introduction

At temperatures above 460K, the intermetallic compound  $\text{PtGa}_2$  forms a pseudobinary system with GaAs, whereas elemental Pt reacts chemically with GaAs to form more stable product compounds.<sup>1</sup> Although  $\text{PtGa}_2$  is supposed to be a high temperature phase and only a metastable species at room temperature, it is actually quite robust. Single crystals and thin films of  $\text{PtGa}_2$  can be grown and examined over the course of years without perceivable disproportionation. Therefore, the study of the electronic and magnetic properties of  $\text{PtGa}_2$  is important for understanding its behavior as a potential conducting contact or an active component in optoelectronic circuitry.

$\text{PtGa}_2$  has the cubic fluorite structure, and is isostructural with  $\text{AuX}_2$  ( $\text{X}=\text{Al}, \text{Ga}, \text{In}$ ). Jan and Pearson<sup>2</sup> have reported that  $\text{AuGa}_2$  is anomalous in the sense that its thermopower is negative at "low" and "high" temperatures while  $\text{AuAl}_2$  and  $\text{AuIn}_2$  have positive thermopowers in the temperature range measured (2 to 300K). The  $^{71}\text{Ga}$  Knight shift and the magnetic susceptibility of  $\text{AuGa}_2$  are strongly temperature-dependent in comparison to its Al and In analogues.<sup>3</sup> On the other hand, resistivity<sup>2,4</sup> and specific heat<sup>5</sup> measurements display no anomalous variation with temperature in  $\text{AuGa}_2$ . In Switendick and Narath's nonrelativistic augmented plane wave (APW) band structure calculation,<sup>6</sup> a flat band ( $\Gamma_2-X_3$ ) lies about 1eV below  $E_F$  in  $\text{AuGa}_2$ , while for  $\text{AuAl}_2$  and  $\text{AuIn}_2$  this band disperses strongly and crosses  $E_F$ . Kim et al.,<sup>7</sup> who included the spin-orbit interaction in their mixed-basis band structure interpolation scheme (MBBIS) calculation, reproduced this result. It is generally believed that this flat  $\Delta_2$  band, derived from Ga 4s-like anti-bonding states, is responsible for the  $\text{AuGa}_2$  anomalies discussed above. However, the observation that the magnetic susceptibility of  $\text{AuGa}_2$  between 4.2 and 300K shows a decreasing diamagnetism with decreasing T is still an unresolved issue.<sup>8</sup> In an angle-resolved photoemission spectroscopy (ARPES) study of  $\text{AuGa}_2$ ,<sup>9</sup> no peak was observed corresponding to the  $\Delta_2$  band, although such a flat band should yield an extremely high density of initial states to be sampled.



Availability	
Availability codes	
Availability	
Dist	Special
A-1	

The MBBSIS was recently utilized to obtain a semiempirical band structure of PtGa<sub>2</sub>.<sup>10</sup> The flat  $\Delta_2$  band was also present in this semiempirical band structure, because the AuGa<sub>2</sub> parameters were used as the starting point in the fit of the DOS to an X-ray photoemission spectrum of the PtGa<sub>2</sub> valence band. However, the <sup>71</sup>Ga Knight shift of PtGa<sub>2</sub> is positive and temperature independent, and the conductivity exhibits no anomalous behavior between 4.2 and 300K.<sup>11</sup> Since there is no first-principles band structure calculation and very little experimental data published for PtGa<sub>2</sub>, the present study was initiated to provide more information about this potentially interesting material. Section II of this paper describes the experimental procedure. In Sec. III, the results are presented and discussed, and Sec. IV concludes this paper.

## II. Experimental procedure

Samples used for the susceptibility measurements were small pieces, with a total weight of 115.4mg, crushed from a PtGa<sub>2</sub> single crystal.<sup>12</sup> A Faraday method, utilizing a Cahn balance, was used for the static magnetic susceptibility measurement in a field of 9 kOe. Temperatures from 4.2 to 300K were measured with calibrated carbon-glass and platinum resistors. In order to verify that the observed magnetization was linear in magnetic field, the susceptibility was measured at several field values at room temperature, liquid nitrogen temperature and liquid helium temperature. The uncertainty in  $\chi$  is less than 1%.

For the electrical resistivity and thermoelectric power measurements, the same single crystal was cut with a wire saw into a long slice of roughly  $10 \times 1 \times 0.5$  mm<sup>3</sup> in size. It was then polished with 5 micron diamond grit and cleaned with acetone just before loading into the dewar. The electrical resistivity was measured with a four-probe method. The thermopower was measured between 4.2 and 300K by establishing a temperature gradient across the sample and measuring the voltage developed against Au leads. The Seebeck coefficient (S) was obtained from the slope of a linear least-squares fit of a series of 30 Seebeck voltage vs. thermal gradient measurements. The absolute Seebeck coefficient was derived after subtracting out the contribution of the Au lead wires from the resultant slope. The uncertainty in S is less than 2.5%.

For the specific heat measurements, a PtGa<sub>2</sub> single crystal was cut to about 10×5×1 mm<sup>3</sup> in size and polished with 5 micron alumina grit. The weight of the sample was 773.9mg. The ripple method<sup>13</sup> used in the heat capacity measurements will be described elsewhere.

### III. Results and Discussion

#### A. Electrical Resistivity

Fig. 1 shows the electrical resistivity of PtGa<sub>2</sub>; there is no anomaly in the  $\rho$  vs. T curve, in agreement with the observation reported in Ref. 11. The room temperature resistivity of PtGa<sub>2</sub>, which is only about eight times larger than that of Au, is compared with those of AuGa<sub>2</sub> and Au in Table 1. Compared with the room temperature electrical resistivity values of WSi<sub>2</sub> (35-60  $\mu\Omega$ -cm)<sup>14</sup> and TaSi<sub>2</sub> (40  $\mu\Omega$ -cm)<sup>15</sup>, which have been suggested as high temperature non-reactive contacts on GaAs, PtGa<sub>2</sub> is a rather good metal and perhaps to be preferred as a contact for devices. However, the residual resistivity ratio ( $\rho_{297.5K}/\rho_{4.2K}$ ) is only 3.34, which indicates that there are impurities or vacancies in the material. These impurities may also be responsible for the low temperature behavior of S and C<sub>p</sub>, as will be discussed in parts (C) and (D) of this section.

#### B. Magnetic Susceptibility

The measured magnetic susceptibility at 9 kOe is shown in Fig. 2. For PtGa<sub>2</sub>,  $\chi$  has two contributions: one is the temperature-independent diamagnetic susceptibility from the Pt- and the Ga-ion core electrons ( $\chi_i^{Pt}$  and  $\chi_i^{Ga}$ ), and the other is the conduction electron susceptibility ( $\chi_e$ ). The expression for  $\chi_e$  also has two components: one is the paramagnetic Pauli susceptibility ( $\chi_e^p$ ), and the other is the Landau-Peierls diamagnetic susceptibility ( $\chi_e^d$ ). For noninteracting free electrons at OK,  $\chi_e^p$  and  $\chi_e^d$  are given by

$$\chi_e^p = \mu_B^2 n(E_F) \quad (1)$$

and

$$\chi_e^d = -\frac{1}{3} \mu_B^2 \left( \frac{m_0}{m^*} \right)^2 n(E_F) \quad (2)$$

where  $\mu_B$  is the Bohr magneton,  $n(E_F)$  is the DOS at  $E_F$  for both spin directions, and  $m^*/m_0$  is the effective mass ratio. The estimated values for  $\chi_i^{\text{Pt}}$  and  $\chi_i^{\text{Ga}}$  are  $-28 \mu\text{emu/mole}^{16}$  and  $-9.54 \mu\text{emu/mole}^{17}$  respectively. The net ionic diamagnetism for  $\text{PtGa}_2$  is therefore  $-47.08 \mu\text{emu/mole}$ . Taking  $m^* = m_0$  in Eq. (2) and extrapolating  $\chi$  to OK, we get  $n(E_F) = 1.40$  electrons of both spin directions/eV-unit cell, which is 22% larger than the value calculated by the MBBSIS<sup>10</sup>. In general, electron-electron interactions lead to an enhancement of the Pauli term by a factor  $(1 - \alpha)^{-1}$ , where  $\alpha$  is the Stoner enhancement parameter. Using the  $n(E_F)$  value from the MBBSIS calculation in the Pauli and the Landau-Peierls terms, we estimate  $\alpha$  to be around 0.16. Since  $\alpha$  usually lies in the range of 0.1 to 0.5,<sup>18</sup> this means that electron-electron interactions in  $\text{PtGa}_2$  are very weak. This in turn justifies the use of the free electron approximation in the above calculation of  $n(E_F)$ .

### C. Thermoelectric Power

The  $S$  vs.  $T$  curve of  $\text{PtGa}_2$  is shown in Fig. 3 along with those of Au and of  $\text{AuGa}_2$ . Below 12K  $S$  of  $\text{PtGa}_2$  becomes negative. This can be attributed to trace magnetic impurity scattering, which has also been observed in Au.<sup>19</sup> The shape of the  $S$  vs.  $T$  curve of  $\text{PtGa}_2$  is very similar to that of Au, although their magnitudes differ. This suggests that there may be some similarities in their conduction mechanisms and topology of their Fermi surfaces. As has already been pointed out,<sup>10</sup>  $\text{PtGa}_2$  has an Au-like DOS, which explains the gold color of this inter-metallic compound.

Since  $S$  of  $\text{PtGa}_2$  remained positive at the highest temperature measured, the electrical conduction is by holes.<sup>20</sup> This behavior is different from that of  $\text{AuGa}_2$ . The calculated flat  $\Delta_2$  band of  $\text{PtGa}_2$ , which is located within 0.1eV of  $E_F$  in the  $\Gamma$ -X direction in the MBBSIS, may actually be either above  $E_F$  or may disperse more strongly and cross  $E_F$ , as in the case of  $\text{AuAl}_2$  and  $\text{AuIn}_2$ . The Knight shift<sup>11</sup> and magnetic susceptibility data support this suggestion, but to be sure about this point a high resolution ARPES study should be performed.

The occurrence of a maximum in Fig. 3 for the thermopower of  $\text{PtGa}_2$  is attributed to the phonon-drag effect.<sup>19</sup> The contribution of this electron-phonon scattering process to  $S$  being

positive implies a dominance of Umklapp over normal processes. For PtGa<sub>2</sub>, the temperature of this maximum ( $T_{\max}$ ) is 37.4K, and therefore  $\theta_D$  is estimated to be  $5T_{\max}=187\text{K}$ .<sup>21</sup> The values of  $\theta_D$  for Au, AuGa<sub>2</sub>, and PtGa<sub>2</sub> determined by various methods are presented in Table 1.

For  $T \geq \theta_D$ , impurity scattering is negligible compared with thermal scattering and the phonon-drag contribution to  $S$  is rather small. Hence, diffusion thermopower ( $S_d$ ) dominates. For metallic conduction,  $S_d$  varies linearly with  $T$ ,<sup>22</sup> and the free electron expression is:<sup>23</sup>

$$S_d = \left( \frac{\pi^2 k_B^2 n(E_F)}{3Ne} \right) T, \quad (3)$$

where  $N$  is the number of electrons per unit cell,  $e$  is the electron charge,  $k_B$  is the Boltzmann constant, and  $n(E_F)$  is the DOS at  $E_F$ .

The dashed line in Fig. 3, which has a slope  $(1.035 \pm 0.083) \times 10^{-8} \text{ V/K}^2$ , is the least-squares fit to the data points for  $T > 187\text{K}$  for PtGa<sub>2</sub>. This linear dependence of  $S$  with  $T$  shows that PtGa<sub>2</sub> is metallic for  $T > \theta_D$ . Comparing with Eq.(3) and using  $N=3$ , one may determine that  $n(E_F) = 1.27$  electrons of both spin directions/eV-unit cell, which is presented in Table 1 along with those of Au and AuGa<sub>2</sub>. The  $N=3$  configuration has been used and justified in certain superconducting compounds containing Ga.<sup>24,25</sup> Pauling<sup>26</sup> assigned effective metallic valences of 6 and 3.5 for Pt and Ga, respectively, when they are bonded in intermetallic compounds. The total number of electrons in one unit cell of PtGa<sub>2</sub> is 16 (10 from Pt and 3 from each Ga), and, from simple addition of valence, 13 of them are used to form the Pt-Ga bonds. Therefore, the number of free electrons in one unit cell of PtGa<sub>2</sub> is 3. This explains qualitatively the assignment of  $N=3$ .

#### D. Specific Heat

Displayed in Fig. 4 are  $C_p$  vs.  $T$  data for PtGa<sub>2</sub> for  $0.46\text{K} \leq T \leq 4.21\text{K}$  and, in the inset,  $C_p/T$  vs.  $T^2$  for  $2.34\text{K} \leq T \leq 4.21\text{K}$ . At low temperature the specific heat of a metal is represented by an equation of the form:

$$C_p(T) = \gamma T + \beta T^3, \quad (4)$$

where  $\gamma$  and  $\beta$  are the coefficients for the electronic and lattice contributions, respectively, to  $C_p$ . If we neglect electron-phonon enhancement, then  $n(E_F) = 3\gamma/k_B^2\pi^2$  and  $\theta_D = (12\pi^4 k_B N_A N_u / 5\beta)^{1/3}$ , where  $N_A$  is Avogadro's number and  $N_u$  is the number of atoms in a formula unit ( $N_u = 3$  for  $\text{PtGa}_2$ ). The data points in the inset of Fig. 4 have been fitted with Eq. (4), yielding the values of  $n(E_F) = 0.32$  states/eV-unit cell and  $\theta_D = 402\text{K}$ . This  $n(E_F)$  value is much smaller than the values obtained from the band structure calculation, the magnetic susceptibility, and the thermopower measurements. This apparent smearing of the DOS at  $E_F$  may be caused by a temperature-dependent DOS at  $E_F$  or/and a contribution arising from magnetic impurities in  $\text{PtGa}_2$ . The latter possibility is supported by the resistivity and the thermopower data presented in this paper, while the former is still an open question.

The lattice constants of Au,  $\text{AuGa}_2$ , and  $\text{PtGa}_2$  are  $4.08 \text{ \AA}$ ,  $6.06 \text{ \AA}$ , and  $5.911 \text{ \AA}$ , respectively.<sup>9,10</sup> Thus, the Brillouin zones for  $\text{AuGa}_2$  and  $\text{PtGa}_2$  have a smaller volume in reciprocal space than for Au. The  $n(E_F)$  value of  $\text{PtGa}_2$  should be closer to that of  $\text{AuGa}_2$  and higher than that of Au, which is confirmed by the  $\chi$  and  $S$  measurements. Rayne<sup>5</sup> reported the specific heat data of  $\text{AuGa}_2$  between 1.4K and 4.2K and found a considerable curvature in the  $C_p/T$  vs.  $T^2$  curve, which, he presumed, is a result of the low  $\theta_D$  and an anomalously high phonon dispersion for the fluorite structure. In order to take into account this curvature, he added a  $T^5$  term in the expression for  $C_p(T)$ , which comes from the second term in the expansion of the phonon spectrum. We observed an upturn at  $T \cong 2\text{K}$  in  $\text{PtGa}_2$ , which is similar to that found in  $\text{AuGa}_2$  by Rayne.<sup>5</sup> By fitting Eq. (4), with the addition of a  $T^5$  term, to  $\text{PtGa}_2$  data down to  $T = 1.4\text{K}$ , we determine  $n(E_F) = 0.51$  states/eV-unit cell and  $\theta_D = 108\text{K}$ . These values are the highest and the lowest obtained for  $n(E_F)$  and  $\theta_D$ , respectively, from the  $C_p$  data for  $\text{PtGa}_2$ . Thus, although in general  $C_p$  data yield the most reliable values for  $n(E_F)$  of metals, for  $\text{PtGa}_2$  the low temperature anomaly that appears in the  $C_p$  vs.  $T$  data causes the determination of  $n(E_F)$  to be unreliable. Therefore, we have omitted this determination from Table I.

## V. Conclusion

No anomalous behavior was found in the electrical resistivity, the magnetic susceptibility, or the thermoelectric power of PtGa<sub>2</sub>. It has a temperature-independent diamagnetic susceptibility. Neglecting electron-electron interaction and using the free electron approximation, the DOS at E<sub>F</sub> was determined to be 1.40 electrons/eV-unit cell from the  $\chi$  data, which agrees with the previously calculated MBBSIS value to within 22%. The S of PtGa<sub>2</sub> resembles that of Au but not that of AuGa<sub>2</sub>. This suggests that the conduction mechanisms and Fermi surface topology of PtGa<sub>2</sub> are similar to those of Au. PtGa<sub>2</sub> has metallic behavior and the conduction is by holes. The flat  $\Delta_2$  band appearing in AuGa<sub>2</sub> may be above E<sub>F</sub> or may disperse more strongly and cross E<sub>F</sub> in PtGa<sub>2</sub>. Assuming free electron conduction and three conduction electrons per unit cell, the DOS at E<sub>F</sub> calculated from the S data is 1.27 electrons/eV-unit cell, which agrees with the value calculated with the MBBSIS to within 15%.

The specific heat of PtGa<sub>2</sub> behaves anomalously below  $T \cong 2\text{K}$ , which may be the result of a temperature-dependent DOS at E<sub>F</sub> or/and a contribution arising from magnetic impurities. The DOS at E<sub>F</sub> obtained from the C<sub>p</sub> data is much smaller than the value calculated from the MBBSIS or the values obtained from  $\chi$  and S measurements.

## Acknowledgments

We would like to thank R.J. Baughman of Sandia National Laboratories for supplying the PtGa<sub>2</sub> single crystal and J.R. Cooper for technical assistance and helpful comments. We also thank Professors G. Gruner and W.G. Clark of the Solid States Science Center and the Department of Physics, UCLA for allowing us to use their equipment. This research was supported in part by a grant from SDIO/IST, managed by the Office of Naval Research. FLAM was supported in part by the National Science Foundation, Grant DMR-8409390, Solid State Chemistry Program. RSW was supported in part by the Alfred P. Sloan and the Camille and Henry Dreyfus Foundations.

## References

1. R. S. Williams, in *Proc. Intl. Conf. on Semiconductor and Integrated Circuit Technology*, Wang Xiuying and Mo Bangxian, eds. (World Scientific Publ.Co., Singapore, 1986) p. 282.
2. J. -P. Jan and W. B. Pearson, *Phil. Mag.* **8**, 279 (1963).
3. V. Jaccarino, M. Weger, J. H. Wernick, and A. Menth, *Phys. Rev. Lett.* **21**, 1811 (1968).
4. J. T. Longo, P. A. Schroeder, and D. J. Sellmyer, *Phys. Lett.* **25A**, 747 (1967).
5. J. A. Rayne, *Phys. Lett.* **7**, 114 (1963).
6. A. C. Switendick and A. Narath, *Phys. Rev. Lett.* **22**, 1423 (1969).
7. S. Kim, J. G. Nelson, and R. S. Williams, *Phys. Rev.* **B31**, 3460 (1985).
8. G. C. Carter, I. D. Weisman, L. H. Bennett, and R. E. Watson, *Phys. Rev.* **B5**, 3621 (1972); W. W. Warren Jr., R. W. Shaw Jr., A. Menth, F. J. DiSalvo, A. R. Storm, and J. H. Wernick, *Phys. Rev.* **B7**, 1247 (1973).
9. J. G. Nelson, W. J. Gignac, S. Kim, J. R. Lince, and R. S. Williams, *Phys. Rev.* **B31**, 3469 (1985).
10. S. Kim, L.-S. Hsu, and R. S. Williams, *Phys. Rev.* **B36**, 3099 (1987).
11. V. Jaccarino, W. E. Blumberg, and J. H. Wernick, *Bull. Am. Phys. Soc.* **6**, 104 (1961).
12. R. J. Baughman, *Mat. Res. Bull.* **7**, 505 (1972).
13. F. L. A. Machado and W. G. Clark, to be published in *Rev. Sci. Instrum.*
14. D. L. Brors, J. A. Fair, K. A. Monnig, *Proc. 9th Intl. Conf. on Chemical Vapor Deposition 1984*, Cincinnati, OH, USA. (Pennington, NJ, USA: Electrochem. Soc. 1984), p. 275-86.
15. M. T. Huang, T. L. Martin, V. Malhotra, J. E. Mahan, *J. Vac. Sci. Technol.* **B 3**, 836 (1985).
16. E. P. Wohlfarth, *Proc. Leeds Phil. Soc.* **5**, 89 (1948); F. E. Hoare and J. C. Matthews, *Proc. Roy. Soc. (London)* **A212**, 137 (1952).
17. C. M. Hurd and P. Coodin, *J. Phys. Chem. Solids* **28**, 523 (1967).
18. R. W. Shaw, Jr. and W. W. Warren, Jr., *Phys. Rev.* **B3**, 1562 (1971).
19. W. J. Pearson, *Solid State Physics (U.S.S.R.)* **3**, 1411 (1961), and references therein.
20. H. Fritzsche, *Solid State Commun.* **9**, 1813 (1971).

21. The relation  $\theta_D \equiv 5T_{\max}$  holds for a lot of metals. See W. B. Pearson, *Ultra-High-Purity Metals* (Metals Park, Cleveland, Ohio: American Society for Metals), p. 201.
22. N. F. Mott and H. Jones, in *The Theory of the Properties of Metals and Alloys*. (Dover: 1958) Ch. VII.
23. D. K. C. MacDonald, in *Thermoelectricity: An Introduction to the Principles*, (John Wiley & Sons: 1962), p.25-6.
24. A. M. Clogston and V. Jaccarino, Phys. Rev. **121**, 1357 (1961).
25. L. F. Mattheiss, Phys. Rev. **138**, A112 (1965).
26. L. Pauling, in *The Chemical Bond*, (Cornell University Press:1967), pp 204-6.

**Table I.** Comparison of values of  $\rho$ ,  $\theta_D$  and  $n(E_F)^a$  for Au, AuGa<sub>2</sub> and PtGa<sub>2</sub>.

	$\rho$ ( $\mu\Omega$ -cm) at 20°C	$\theta_D$ (K)	$n(E_F)$
Au	2.24 <sup>b</sup>	165 <sup>c</sup>	0.31 <sup>d</sup>
		162.4 <sup>e</sup>	0.18 <sup>f</sup>
		161.6 <sup>g</sup>	0.24 <sup>h</sup>
AuGa <sub>2</sub>	12.9 <sup>i</sup>	245 <sup>j</sup>	1.12 <sup>k</sup>
		235 <sup>c</sup>	1.14 <sup>m</sup>
		192 <sup>m</sup>	
PtGa <sub>2</sub>	19.05 <sup>n</sup>	187 <sup>c</sup>	1.09 <sup>f</sup>
			1.27 <sup>o</sup>
			1.40 <sup>p</sup>

- a. DOS at  $E_F$  in units of number of electrons per eV per unit cell for both spin directions.
- b. Handbook of Chemistry and Physics (College Edition), (Chem Rubber Co.: 1984), p. F-120.
- c. Estimated from thermoelectric power measurements,  $\theta_D \cong 5 T_{\max}$ .
- d. Calculated from D. L. Martin's specific heat data (Phys. Rev. **141**, 141 (1966)) using  $n(E_F) = 3 \gamma / k_B^2 \pi^2$ , where  $\gamma$  is the intercept of the  $C_p/T$  vs.  $T$  curve.
- e. From specific heat measurement, D. L. Martin, Phys. Rev. **141**, 141 (1966).
- f. From MBBSIS band structure calculation, Ref. 10.
- g. From zero-temperature elastic constants measurement, G. A. Alers, in *Physical Acoustics*, W. P. Mason, ed. (Academic Press Inc., New York), Vol. IIIB, Chap. I.
- h. Calculated from thermoelectric power data, Ref. 16, at  $T > \theta_D$  using Eq. (3) in this paper and  $N=1$ .
- i. From resistivity measurement, Ref. 2.
- j. Calculated in Ref. 5 from the resistivity data of Ref. 2.
- k. From MBBSIS band structure calculation, Ref. 7.
- m. From specific heat measurement, Ref. 5.
- n. From resistivity measurement, this work.
- o. From thermoelectric power measurement, this work.
- p. From magnetic susceptibility measurement, this work.

## FIGURE CAPTIONS

- Fig. 1.** Electrical resistivity of PtGa<sub>2</sub> as a function of temperature from 4.2 to 300K.
- Fig. 2.** Magnetic susceptibility of PtGa<sub>2</sub> and AuGa<sub>2</sub> as a function of temperature from 4.2 to 300K. The AuGa<sub>2</sub> data were taken from Ref. 3.
- Fig. 3.** Temperature dependence of the thermoelectric power  $S(T)$  for Au, AuGa<sub>2</sub>, and PtGa<sub>2</sub>. The data for Au and AuGa<sub>2</sub> are taken from Ref. 12 and Ref. 2, respectively. The dashed line is the least-squares fit to PtGa<sub>2</sub> data for  $T > 187\text{K}$ .
- Fig. 4.** Specific heat  $C_p$  vs. temperature  $T$  for PtGa<sub>2</sub> for  $0.46\text{K} \leq T \leq 4.21\text{K}$ . Inset:  $C_p/T$  vs.  $T^2$  for  $2.34\text{K} \leq T \leq 4.21\text{K}$ . The solid line represents a least-squares fit of Eq. (4) in the text to the data.

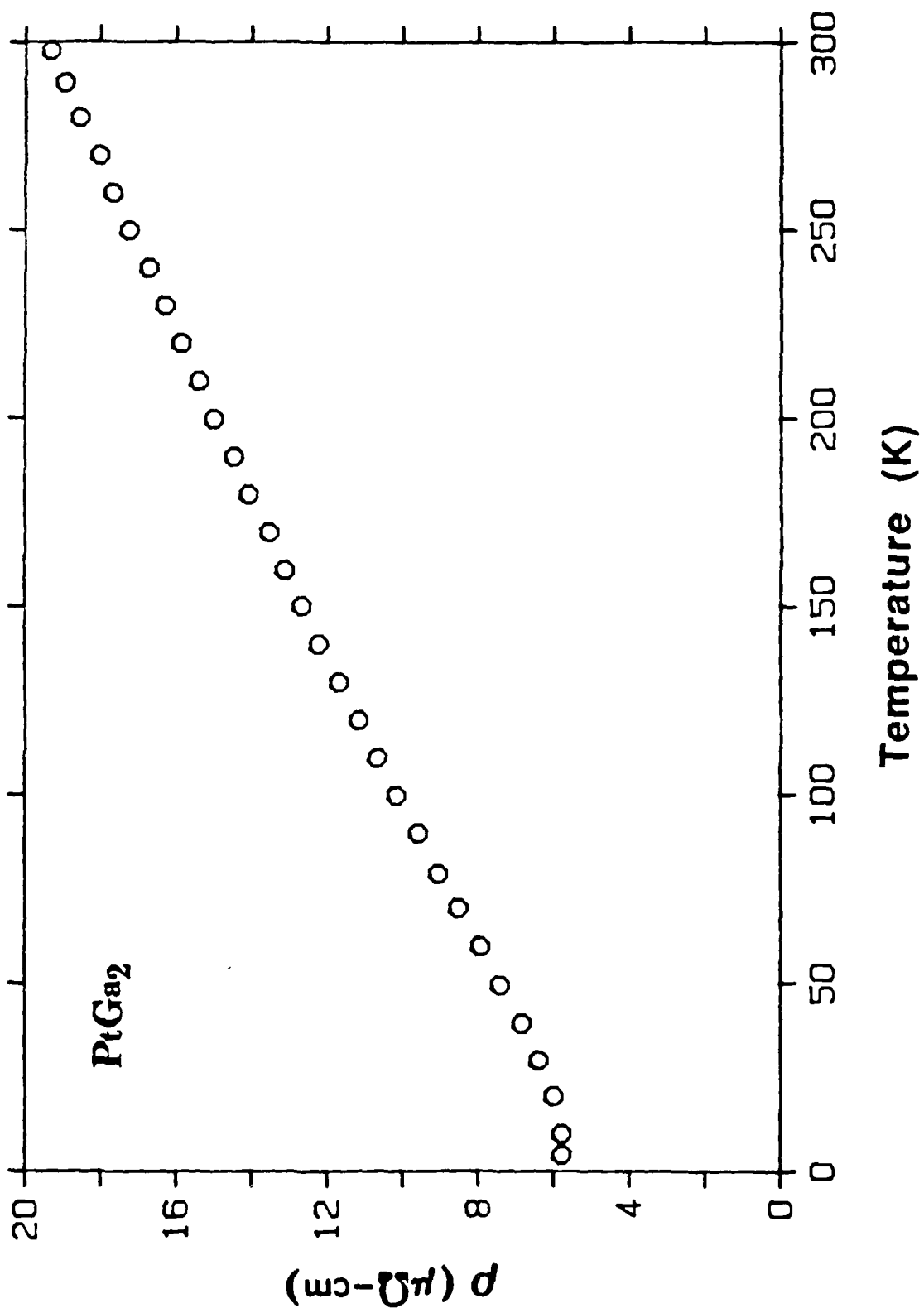


FIG. 1

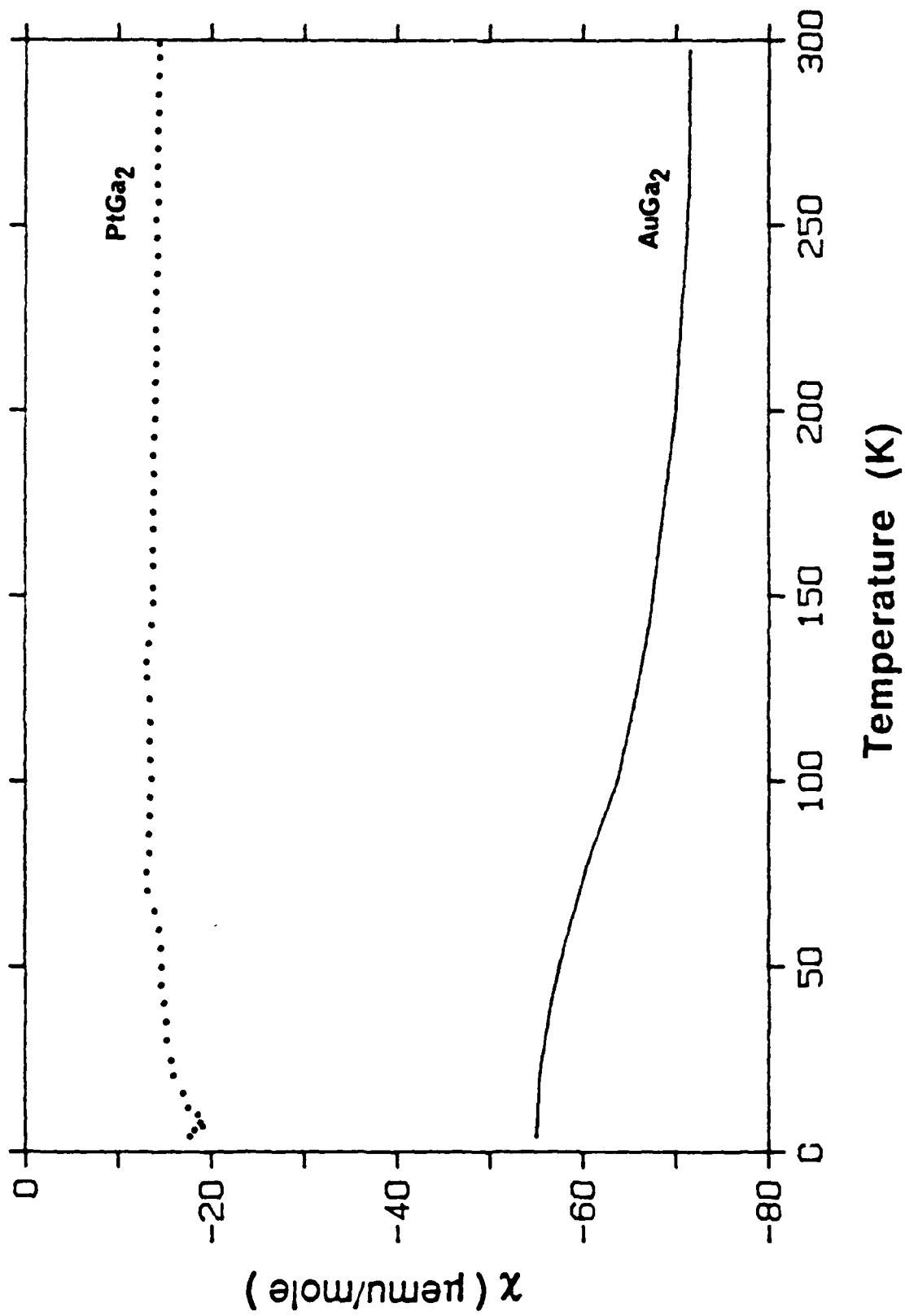


FIG. 2

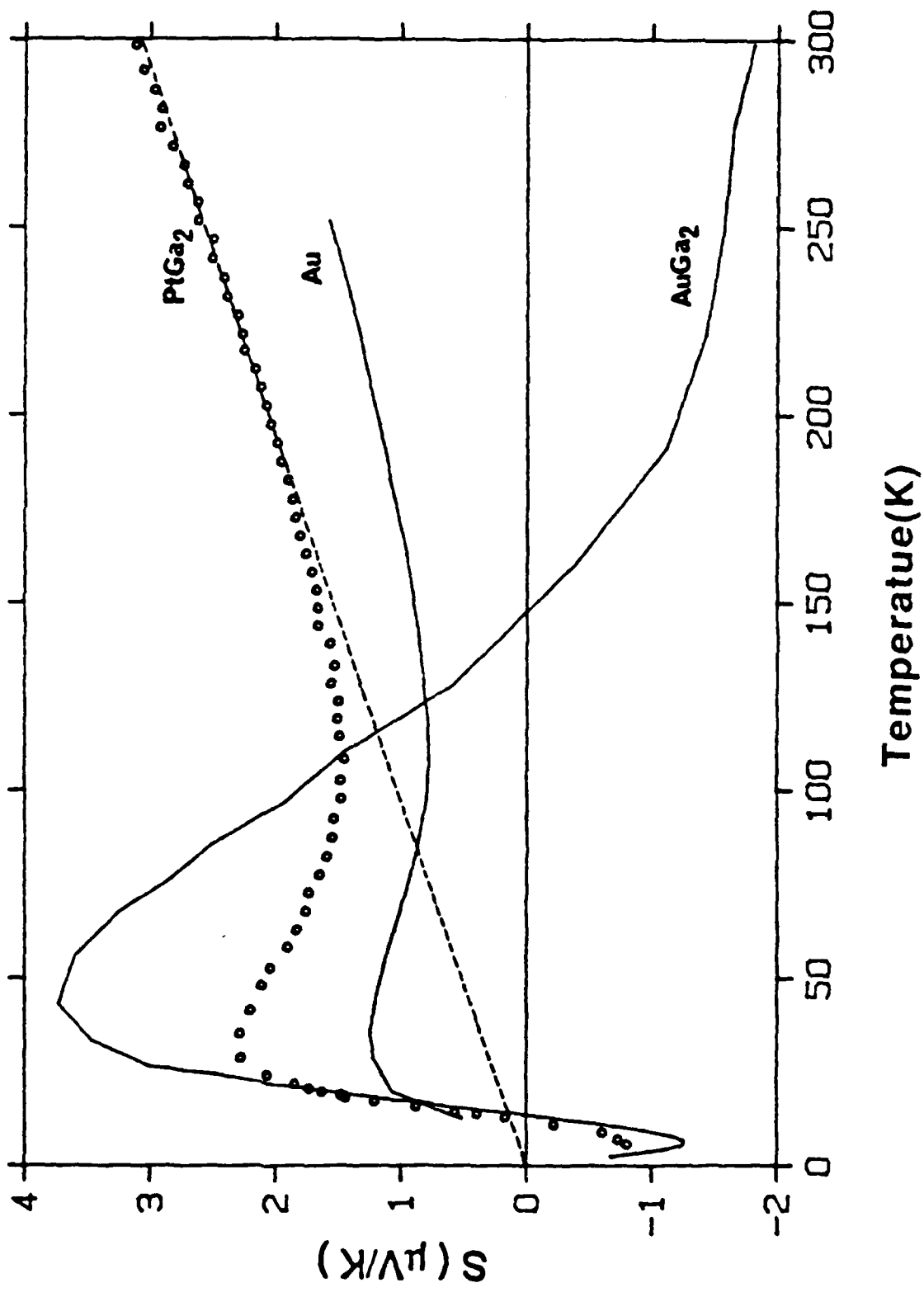


FIG. 3

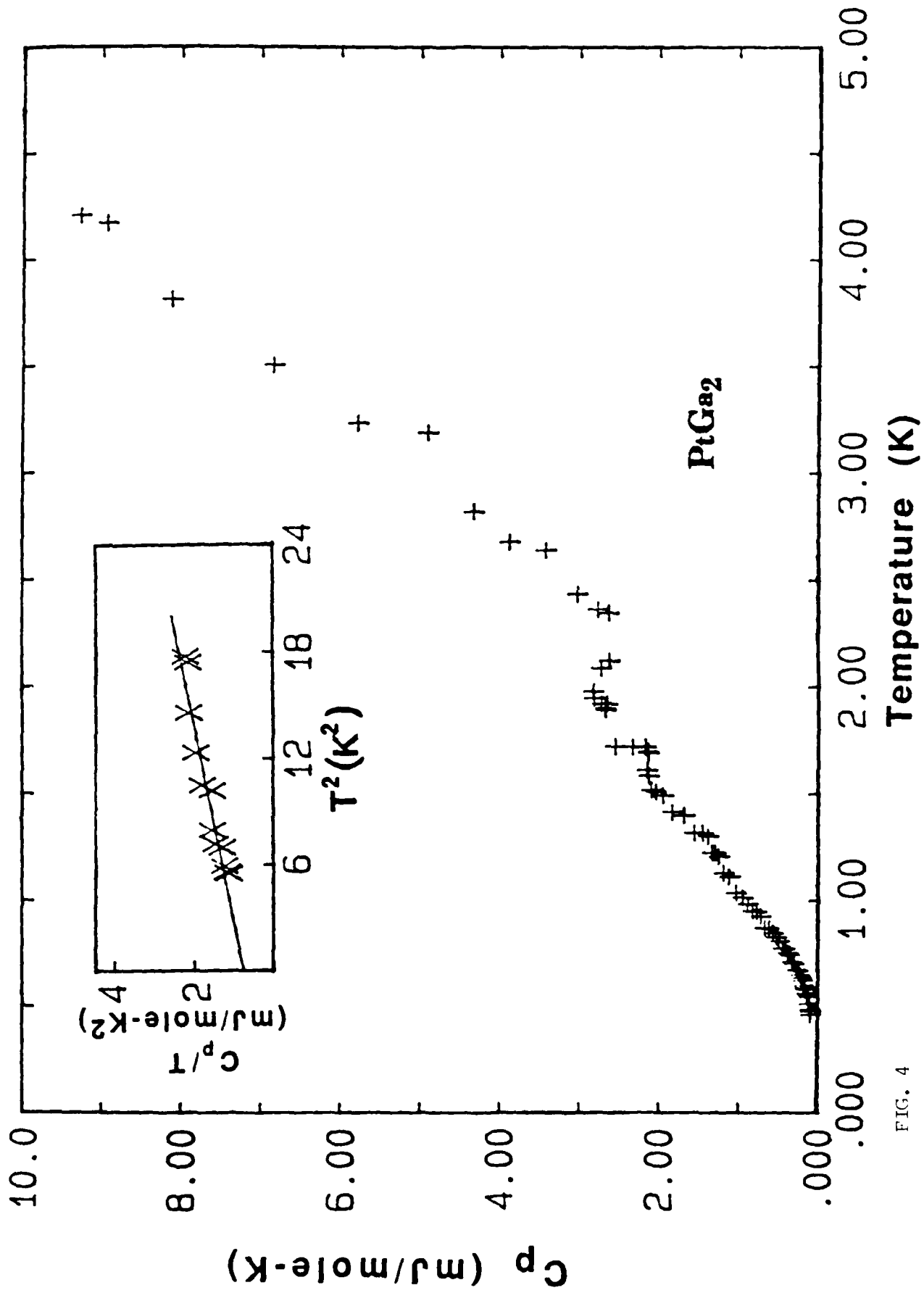


FIG. 4